Geologica Acta, Vol.11, Nº 4, December 2013, 483-493
DOI: 10.1344/105.000002054
Available online at www.geologica-acta.com

geologica acta

Variations in chemistry of macerals as reflected by micro-scale analysis of a Spanish coal

M. MASTALERZ [1] **J.C. HOWER** [2] **D.N. TAULBEE** [2]

[1] **Indiana Geological Survey, Indiana University**
611 North Walnut Grove Ave., Bloomington, Indiana, 47405-2208, United States.
Phone: 1-812-855-9416. E-mail: mmastale@indiana.edu

[2] **University of Kentucky Center for Applied Energy Research**
2540 Research Park Drive, Lexington, Kentucky 40511, United States.
Hower phone: 1-859-257-0261 E-mail: james.hower@uky.edu.
Taulbee phone: 1-859-257-0238 E-mail: dntaulbee@uky.edu

ABSTRACT

An Oligocene lignite (Ebro Basin, Spain) and its density fractions were analyzed petrographically and with microscale techniques (electron microprobe and micro-FTIR) to gain insight into differences between individual macerals of low rank high-sulfur coal. The density of the alginite-dominated fraction is below 1.26g/cm^3, and that of the huminite-dominated fraction is above 1.38g/cm^3. Densities within 1.26-1.38g/cm^3 represent mixtures of liptinite and huminite macerals. With regard to elemental composition, alginite has the highest carbon content (75.6% on average) and the lowest oxygen content (6.1% on average). Corpohuminite is characterized by the lowest carbon content (62.3% on average) and the highest oxygen content (21.5% on average). Nitrogen contents for corpohuminite and ulminite (~1%) are similar, but are significantly lower in alginite (0.2% on average). Sulfur content is highest in alginite (13.4% on average), followed by corpohuminite (9.8%) and ulminite (7.7%). Functional group analysis documents large differences between macerals of the huminite and liptinite group, but also indicates differences between individual macerals within both the huminite and liptinite group. These differences are most notable in aromaticity, degree of aromatic ring condensations, and hydrocarbon potential.

KEYWORDS | **Lignite. Macerals. Elemental composition. Functional groups.**

INTRODUCTION

The late Oligocene Mequinenza lignite is found in the eastern Ebro Basin of northeast Spain (Fig. 1). Detailed geologic descriptions of the coal and its setting are found in Cabrera and Saez (1987), Querol *et al.* (1996), Arenas *et al.* (1999), and Cabrera *et al.* (2002). Briefly, the Ebro Basin is a foreland basin of the Pyrenees that between early Oligocene and the late Neogene was filled with nonmarine sediments. Sedimentary environments included large alluvial fans, fluvial systems along tectonically active basin margins, and shallow lacustrine systems that include both evaporitic sediments and lignite beds. The lignite deposits have, on as-received-basis, high ash (30-35% on average) and very high sulfur (3-8% on average) contents, and the heating value ranges from 14.6 to 23.0kJ kg^{-1} (Cabrera and Saez, 1987). Petrographically, these coals are rich in huminite (and corpohuminite, in particular) and have low liptinite and inertinite content (White *et al.*, 1994; Querol *et al.*, 1996). They were deposited in a lacustrine environment ranging in salinity from fresh to saline, as indicated by biomarker studies (Cabrera *et al.*, 2002).

The present study provides details of the chemistry of individual macerals in the lignite. Because of the very high sulfur content (Chou, 2012), this coal provides a rare opportunity to discuss the effect of the abundance of sulfur on maceral chemistry. Both bulk lignite and Density-Gradient-Centrifugation (DGC) separated fractions were analyzed using standard petrographic and in-situ microscale (electron microprobe and micro-FTIR) techniques.

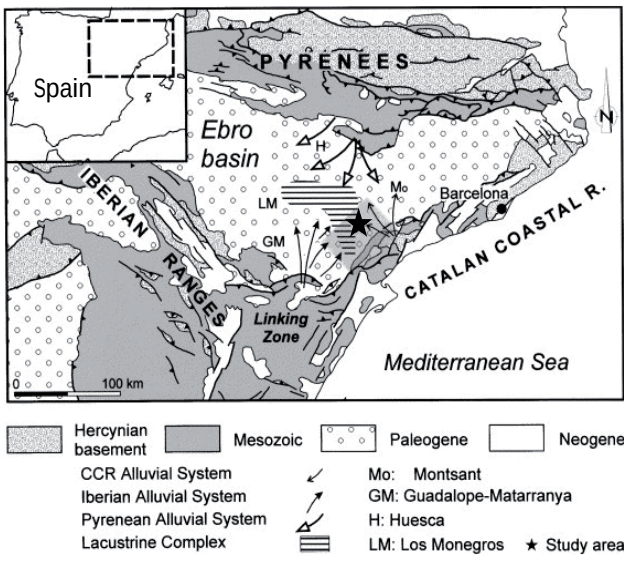

FIGURE 1 | Location of the Ebro Basin in Spain. Star in the eastern part of the Ebro Basin indicates the location of the lignite studied. Alluvial systems, H: Huesca, GM: Guadalope-Matarranya, LM: Los Monegros, and Mo: Montsant. Modified after Cabrera et al. (2002).

METHODS

Density-gradient centrifugation

A sample of the lignite from the eastern Ebro Basin in Spain (obtained from Colin Snape, University of Nottingham; at University of Strathclyde at time of sample procurement) was crushed to <100 mesh, demineralized by HF, and separated by density-gradient centrifugation. This technique is based on procedures developed by Dyrkacz *et al.* (1981, 1991) and modified by Robl *et al.* (1987). A Beckman model J2-21 centrifuge with a 1900-ml Titanium JCF-Z zonal core rotor, located at the University of Kentucky Center for Applied Energy Research, was used for the DGC separation. For each run, an ultrasonically dispersed mixture containing of about 8g of the coal, 200ml of water, and 2.0+/-0.05g of Brij-35 surfactant was pumped to the outer wall of the centrifuge rotor. After centrifugation at up to 25,000G's on the outer wall, Fluurinert (3M Corp.), a high-density, water-immiscible fluorocarbon was used to force the density gradient from the rotor and through a density meter. The fractions were filtered under vacuum through a 0.45-μm filter, rinsed, dried overnight at 60ºC, and weighed. Multiple runs were performed to obtain sufficient amounts of material for further analysis.

Petrology

Fractions of the density-gradient-centrifugation separates were mixed with epoxy in 2.54cm molds and prepared to a final 0.05μm polish for examination on a Leitz Orthoplan microscope using a 50x, oil-immersion, reflected-light objective and 10x eyepieces. Vitrinite reflectance was measured using a Zeiss Photoscope microscope.

Micro-FTIR spectroscopy

Micro-FTIR measurements were performed on polished blocks using a Nicolet 6700 spectro-photometer connected to a Nicolet Continuum microscope operated in reflectance mode. The microscope was linked to a liquid-nitrogen-cooled mercury-cadmium-telluride (MCT) detector (Nicolet Instrumentations Inc., Madison, WI, USA) and a computer-controlled mapping stage. Micro-FTIR spectra were obtained at a resolution of 4cm^{-1}, using a gold plate as background. The 15x infrared objective and the measuring aperture of 100 x 100μm were used in most cases, except for sporinite and cutinite, the small size of which required the use of a 32x objective and apertures suitable for these macerals. The OMNIC program was used for spectral de-convolution, curve-fitting, and determination of peak integration areas. All micro-FTIR spectra were subjected to Kramers-Kroning transformation, and the peak

TABLE 1 | FTIR-derived ratios used in this study

Parameter	Wavenumber range (cm^{-1})	Functional groups
Aromaticity AR1	3000-3100/2800-3000	Aromatic stretching C-H/Aliphatic stretching C-H
Degree of aromatic ring condensation (DAC)	700-900/1550-1650	Aromatic out-of-plane C-H/Aromatic carbon C=C
Aliphatic chain length (ACL)	2900-3000	CH_2/CH_3 in aliphatic stretching region
Hydrocarbon potential (FA)	2930+2860/(2930+2860+1600)	CH_2 in aliphatic stretching/CH_2 in aliphatic stretching +aromatic carbon C=C
Oxidation index Ox1	1715/2800-3000	Oxygenated groups/ Aliphatic stretching C-H
Oxidation index Ox2	1715/1550-1650	Oxygenated groups/ Aromatic carbon C=C

assignments of spectra were based on previously published work on coals (Painter *et al.*, 1985; Wang and Griffiths, 1985; Mastalerz and Bustin, 1993).

For semi-quantitative FTIR analysis, many indices are used to evaluate the chemical characteristics of coal macerals (Kister *et al.*, 1990; Mastalerz and Bustin, 1996). The ratios selected for this study are listed in Table 1. Curve-fitting of the ~1560-1800cm^{-1} region peak provided the integration areas of oxygenated and aromatic carbon groups. Self-deconvolution of the 2800-3000cm^{-1} region was performed to calculate CH2/CH3 ratios.

Electron Microprobe Analysis

The same polished blocks as used for optical and FTIR analyses were sputter-coated with carbon for use in the microprobe. The samples were analyzed for the abundances of carbon, oxygen, nitrogen, sulfur, iron, calcium, and chlorine using a Cameca SX-100 electron microprobe equipped with four wavelength-dispersive spectrometers. The microprobe provides compositional data in weight percent for each element, based on the total number of elements analyzed. A PC2 crystal was used to measure carbon and oxygen; a PET crystal for sulfur, calcium, and silicon; a PC0 for nitrogen, and an LiF crystal for Fe. Ten-second beam count times were used for C, O, and S, and 20 seconds for N. Detailed procedures for light element determination are found in Bustin *et al.* (1993) and Mastalerz and Gurba (2000). Beam conditions included a beam size of 20μm, a current of 20nA, and an accelerating voltage of 10kV. Depending on the maceral availability and its identification under the probe optics, the number of analyses for individual macerals per sample varied from 5 to 25.

RESULTS AND DISCUSSION

Petrology and maceral density

The original coal sample is composed of huminite group macerals, dominated by a textinite-ulminite mix with corpohuminite, with lesser proportions of sporinite, cutinite, and alginite, and sporadic inertinite macerals (Table 2; Fig. 2). Reflectance of huminite macerals is quite similar, ranging from 0.34 to 0.41% (Table 3). Ulminite and levigelinite have higher reflectance (0.40 and 0.41%, respectively) than corpocollinite and porigelinite (0.36 and 0.34%, respectively).

In density fractions, density progresses from alginite-dominated light fractions (density <1.26g/cm^3, particularly the <1.18g/cm^3 fraction, Table 2) (Fig. 2A, B), through textinite-ulminite/corpohuminite/liptinite/alginite mixes in the intermediate fractions (density 1.26-1.38g/cm^3), and textinite-ulminite-corpohuminite-rich fractions (1.38 -1.43g/cm^3), to almost pure (>93%) textinite-ulminite heavy fractions of 1.43-~1.59g/cm^3 (huminite-rich fractions shown on Fig. 2C-H). In comparison, for Miocene lignite from Indonesia, Stankiewicz *et al.* (1996) obtained densities of 1.43g/cm^3 and above for almost pure huminite, whereas the fraction of 1.10g/cm^3 was liptinite-rich. In that study, density fractions of 1.26 and 1.35g/cm^3 were mixed fractions rich in both huminite and liptinite. This comparison suggests that for coal of low rank, densities of 1.38g/cm^3 and above are characteristic of huminite. Discrepancies between densities of the liptinite-dominated fraction between the Indonesian coals (<1.10g/cm^3) and the Spanish coals studied here (<1.26g/cm^3) may result from compositional differences in liptinite macerals; in the Indonesian coal, liptinite did not include alginite, which is a prominent component of the Spanish coals studied (Table 2). Alginite is not a common component of coal and, therefore, its density in coal has not been studied to the same extent as in shales, where several studies indicated densities below 1.15g/cm^3 (Mastalerz *et al.*, 2012, and references therein). Hower *et al.* (1994) described similar fractionation of a high-volatile A bituminous coal from Kentucky, with liptinite being the most abundant in the <1.17g/cm^3 density fraction (total vitrinite exceeding 98% from the 1.286-1.301g/cm^3 fractions) and fusinite + semifusinite >98% in the >1.388g/cm^3 fractions. For high volatile bituminous Eocene coal from Indonesia, Stankiewicz *et al.* (1996) obtained densities <1.11% for

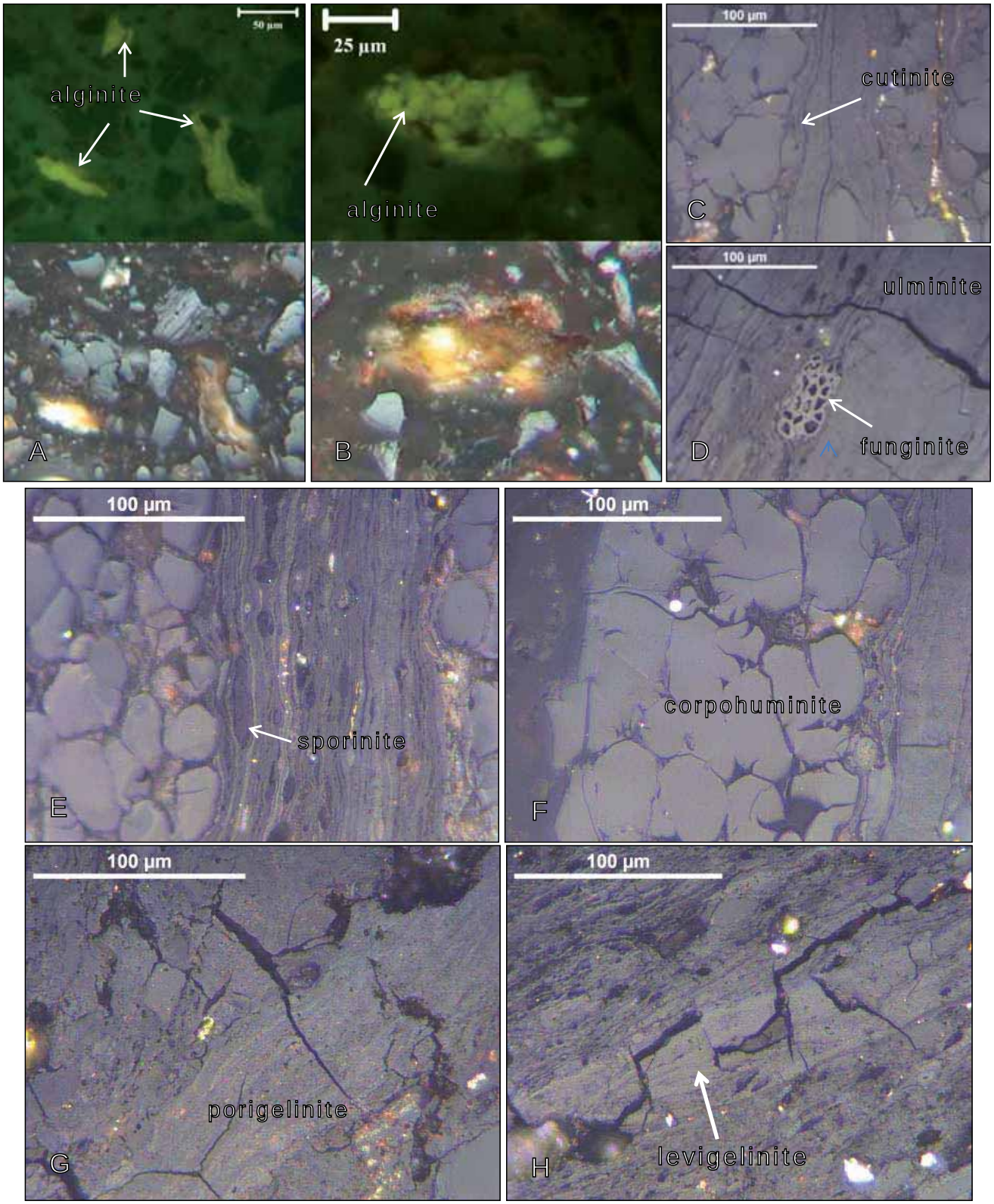

FIGURE 2 | Photomicrographs of the coal macerals studied. A,B) Blue-light (top) and white-light images of alginite. C-G) Reflected light, oil immersion. C) Thin cutinite associated with ulminite and corpohuminite. D) Funginite surrounded by huminite macerals. E) Sporinite associated with ulminite and corpohuminite. F) Corpohuminite. G) Porigelinite. H) Levigelinite.

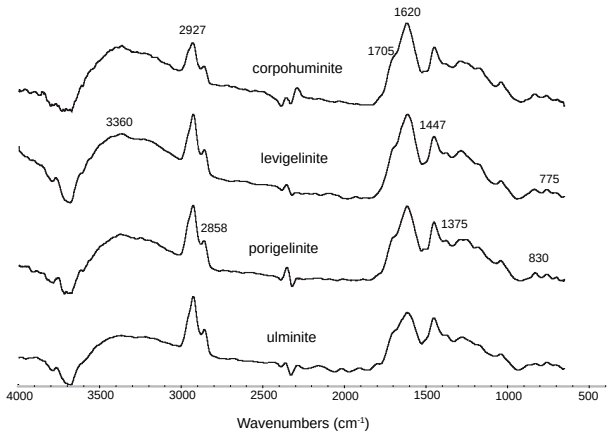

FIGURE 3 | Micro-FTIR spectra of huminite macerals. Each spectrum is an average spectrum based on six to ten individual spectra.

almost pure liptinite (resinite) fractions, and found almost pure vitrinite in the density fractions of 1.25g/cm^3 and above. This comparison, as well as other similar studies on coal (*e.g.* Rimmer *et al.*, 2006) suggest that densities of maceral groups can shift slightly in response to rank, specifics of macerals composition within maceral groups, and possibly other factors such as, for example, the type of original vegetation.

Distribution of functional groups

Several macerals of the huminite group were analyzed using micro-FTIR and they include ulminite, corpohuminite, levigelinite, and porigelinite (Fig. 3). Micro-FTIR spectra of each maceral were obtained both on the bulk lignite and density fractions and several spectra were used to generate the average spectrum that was used for interpretation. Qualitatively, spectra of huminite macerals look similar (Fig. 3), being characterized by prominent bands in the aliphatic stretching region (2800-3000cm^{-1}), aromatic carbon region (peak at 1620cm^{-1}), and aliphatic bending region (1350-1460cm^{-1}). Bands of smaller absorbance occur in the oxygenated group region (peak at 1705cm^{-1}) and aromatic out-of-plane region (700-900cm^{-1}).

In the liptinite group, sporinite, cutinite, and alginite were analyzed using micro-FTIR (Fig. 4). FTIR spectra of sporinite and cutinite were collected on the bulk lignite, whereas the lightest density fraction (1.00-1.18g/cm^3) was used to collect alginite spectra because alginite could not be identified with the dry infrared objective in the bulk coal. This coal has also areas where ulminite was finely interfingered with cutinite; these areas were also analyzed (marked as cutinite-ulminite in Figures 5-7). Inertinite macerals, although present in the coals studied in minor quantities (Figure 2D), either were not identified with certainty using the dry infrared objective or were too small to measure and, therefore, are not discussed in this paper.

Spectra of liptinites (Fig. 4) are very different from those of huminite because they have: i) much more defined and prominent aliphatic stretching bands (2800-3000cm^{-1}); ii) much lower absorbance of aromatic carbon (peak at 1620cm^{-1}); iii) generally well-defined bands of carboxyl/carbonyl at ~1710cm^{-1}; and iv) non-detectable aromatic bands in the aromatic out-of-plane region (700-900cm^{-1}). These are expected differences and result from the aliphatic character of liptinite group macerals in contrast to more aromatic huminite (*e.g.* Mastalerz and Bustin, 1993). While notable differences in spectra exist between macerals of the huminite and liptinite groups, the differences among the macerals within the liptinite group alone are less pronounced upon qualitative inspection of the spectra (Fig. 4). One exception is noted for the cutinite spectrum, which has a prominent aromatic carbon band at ~1610cm^{-1}; this band, however, is from the more aromatic ulminite associated with cutinite in this coal. The spectra of alginite show prominent aliphatic stretching bands, their narrow peaks resulting from an overwhelming contribution of CH2 and a very minor CH3 contribution in this region, which, in turn, suggests long and straight aliphatic chains (Lin and Ritz, 1993).

The latter peaks may also suggest cyclic aliphatics, confirmed by the absence of a peak at 1375cm^{-1} attributed to bending by terminal methyl groups.

The semi-quantitative differences in the ratios of selected functional groups between macerals are shown in

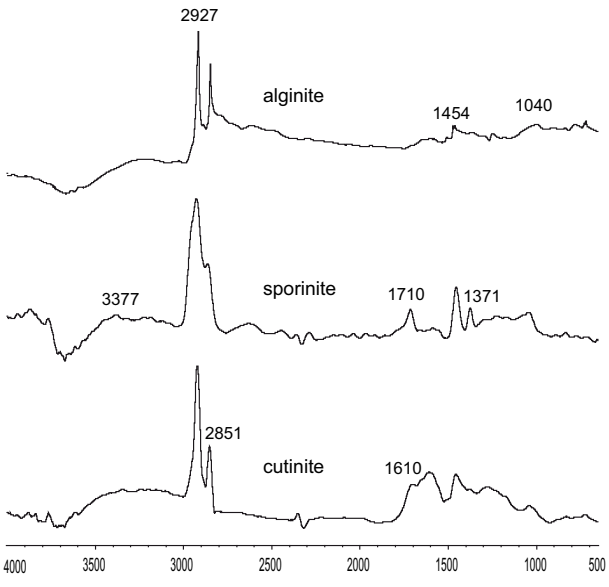

FIGURE 4 | Micro-FTIR spectra of liptinite macerals. Each spectrum is an average spectrum based on six individual spectra.

TABLE 2 | Petrographic composition (in volume %) of the bulk coal and its density fractions. Other liptinite category includes sporinite and cutinite

density	Huminite			Inertinite		Liptinite		
g/cm^3	textinite/ulminite	corpohuminite	detrohuminite	fusinite	semifusinite	alginite	bituminite	Other liptinite
raw coal	60.3	27.7	0.7	0.5	0.2	6.2	0.2	4.2
1.0 to 1.18	5	5	1	0	0	83	0	6
1.18 to 1.22	4	7	2	1	0	78	1	7
1.22 to 1.26	11	6	3	0	0	55	8	17
1.26 to 1.28	3	16	6	0	0	42	5	28
1.28 to 1.30	14	11	6	0	0	29	9	31
1.30 to 1.32	12	28	3	0	0	24	7	26
1.32 to 1.34	18	38	4	0	trace	12	6	22
1.34 to 1.36	24	40	10	0	1	11	3	11
1.36 to 1.38	12	56	7	1	1	6	1	16
1.38 to 1.40	68	29	0	0	1	0	0	2
1.40 to 1.41	23	68	2	1	0	0	0	6
1.41 to 1.42	47	41	0	0	0	3	1	8
1.42 to 1.43	58	34	0	1	0	0	0	7
1.43 to 1.44	93	4	0	0	0	0	0	3
1.44 to 1.45	93	5	0	1	0	0	0	1
1.45 to 1.46	93	4	0	0	1	0	0	2
1.46 to 1.47	95	5	0	0	0	0	0	0
1.47 to 1.48	96	4	0	0	0	0	0	0
1.48 to 1.49	99	trace	0	0	0	0	0	1
1.49 to 1.50	99	1	0	0	0	0	0	0
>1.50	100	0	0	0	0	0	0	0

Figures 5-7. Aromaticity (AR1, Table 1) of the huminite group macerals is higher than that of liptinite (Fig. 5A). Within the vitrinite group, ulminite and corpohuminite have the lowest and highest aromaticity, respectively. Within the liptinite group, sporinite has a higher aromaticity than cutinite and alginite. Increase in aromaticity is accompanied by an increase in maceral reflectance, with correlation coefficient R^2 of 0.50. The degree of aromatic ring condensation (DAC, Table 1) is highest in porigelinite and lowest in sporinite (Fig. 5B), and no correlation existed with maceral reflectance. Hydrocarbon potential (FA, Table 1) is much higher in the liptinite than in the huminite group macerals (Fig. 6A), expectedly revealing a strong negative correlation with maceral reflectance (R^2= 0.82). Within the huminite group this ratio is highest in porigelinite and decreases in this order: porigelinite>ulminite> levigelinite> corpohuminite. Aliphatic chains (ACL, Table 1) are the longest in alginite (Fig. 6B), and there was no correlation with maceral reflectance. Within the huminite group, levigelinite has the longest and least-branched chains and porigelinite the shortest chains. Finally, ratios that utilize oxygenated groups (Fig. 7A, B) show that liptinite group macerals, as compared to vitrinite group macerals, have lower relative contributions of oxygenated groups relative to the aliphatic C-H groups (OX1, Fig. 7A) but higher contribution of oxygenated groups relative to aromatic carbon (OX2, Fig. 7B). The juxtaposition of ulminite material to cutinite results in a rapid decrease in these ratios, although the decrease is likely not characteristic of cutinite itself (Fig. 7A, B). Among huminite group macerals, porigelinite has the highest contribution of oxygenated groups and corpohuminite the lowest. These two ratios that utilize oxygenated groups have strong relationships with maceral reflectance; a positive correlation with R2 of 0.68 exists with OX1, whereas a negative correlation (R2 of 0.96) exists with OX2.

TABLE 3 | Reflectance (R_o) of macerals in the coal studied. Std: standard deviation. n: number of measurements

		R_o (%)	Std	n
Vitrinite group	ulminite	0.40	0.042	25
	corpocollinite	0.36	0.024	25
	levigelinite	0.41	0.025	25
	porigelinite	0.34	0.033	25
Liptinite groups				
	cutinite	0.14	0.006	10
	sporinite	0.14	0.013	15
Inertinite group				
	funginite	0.62	0.013	8
	semifusinite	0.63	0.062	25

While the relationships between maceral reflectance and some functional group ratios (for example aromaticity, AR1, or hydrocarbon potential, FA) are expected based on different maceral chemistries, an interesting observation

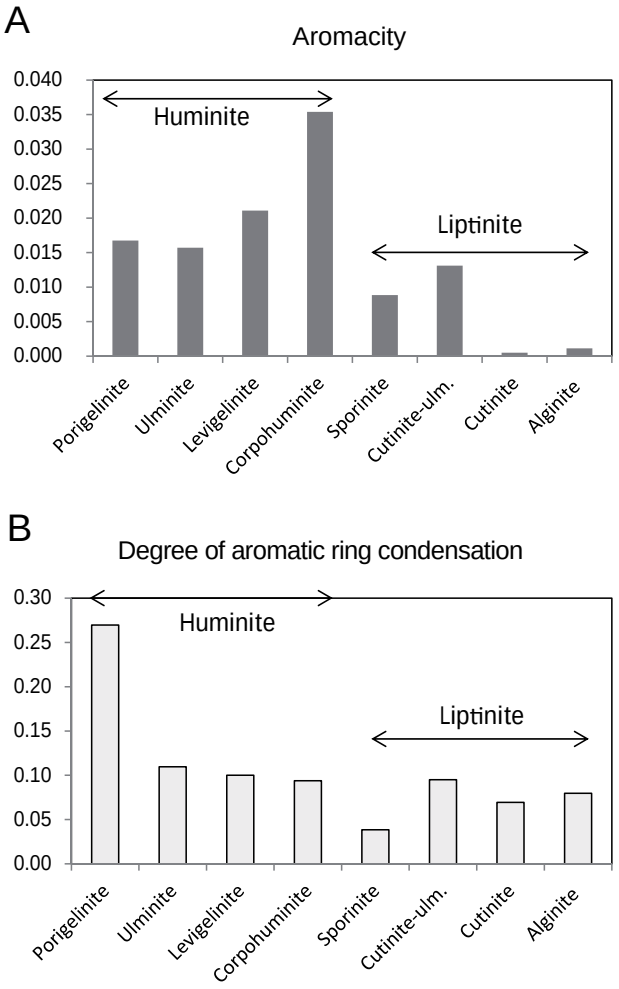

FIGURE 5 | A) Aromaticity and B) degree of aromatic ring condensation of the macerals studied.

for the coal studied is its high contribution of aliphatic groups (both in aliphatic stretching and bending regions) in vitrinite macerals (Fig. 3) at this low rank. This supports the suggestion that high-S coals follow a different evolution path during diagenesis than low sulfur coals, possibly because of replacement of the oxygen by sulfur in the molecular structure and the consequent slower elimination of aliphatic chains during maturation (Li *et al.*, 2010).

Elemental composition

This study also provides information on the elemental chemistry of individual macerals in the low-rank coal. While knowledge of the chemistries of individual macerals in bituminous coals has advanced over last decades, attributable to both maceral separation (Dyrkacz *et al.*, 1984, 1991; Stankiewicz *et al.*, 1996) and in-situ analysis using the electron microprobe (Mastalerz and Bustin, 1993; Gurba and Ward, 2000; Ward *et al.*, 2005), these techniques have not yet been applied to the same degree in lower-rank coals (Drobniak and Mastalerz, 2006; Li *et al.*, 2007, 2010).

The elemental compositions of corpohuminite, ulminite, and alginite macerals for the bulk samples and density fractions in the coal studied are listed in Table 4. Other macerals were difficult to identify under the electron microprobe and, therefore, were not analyzed. Out of the three macerals analyzed, alginite has the highest carbon content (75.6% on average, Table 5) and the lowest oxygen content (6.1% on average). Corpohuminite is characterized by the smallest carbon content (62.3% on average) and the largest oxygen content (21.5% on average). Corpohuminite and ulminite have similar nitrogen contents (~1%), but are significantly lower in alginite (0.2% on average). These are high-sulfur coals and sulfur content is greatest in alginite (13.4% on average), followed by corpohuminite (9.8%) and ulminite (7.7%). In comparison, analysis of ulminite in Polish Miocene lignitic wood (Drobniak and Mastalerz, 2006) results in very similar carbon contents (~64-69%) to that of the ulminite studied (~70%, Table 4). However, the ulminite studied has significantly lower oxygen, higher nitrogen, and significantly higher sulfur contents that the Miocene wood. Those elemental differences are consistent with the very different depositional environments of these two

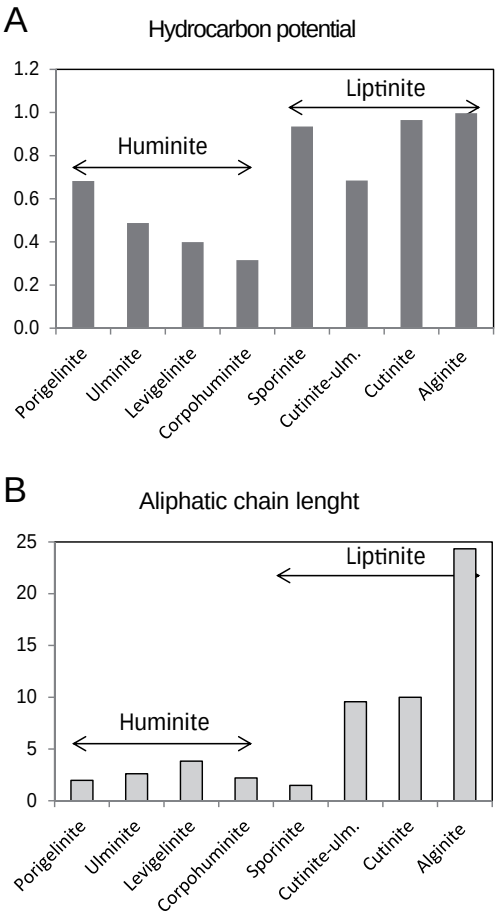

FIGURE 6 | A) Hydrocarbon potential and B) aliphatic chain length of the macerals studied.

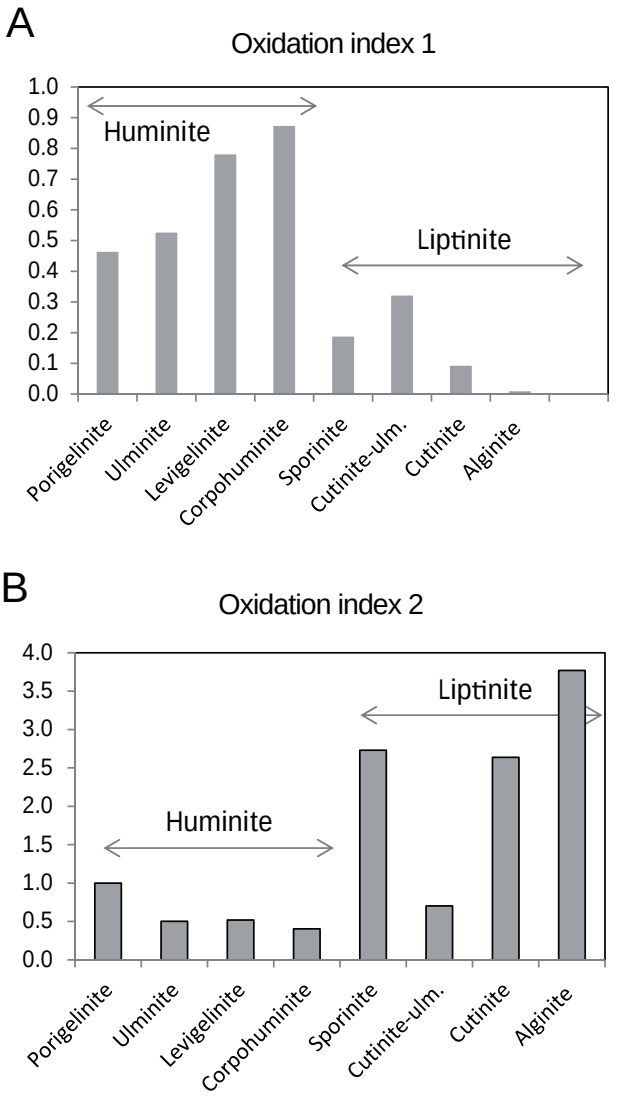

FIGURE 7 | Oxidation indices of the macerals studied.

deposits: freshwater for the Polish deposit (Wagner, 1996) and fresh to saline water for the Spanish deposit (Cabrera *et al.*, 2002). Li *et al.* (2010), based on microprobe and FTIR studies, demonstrated that macerals in high-S coals from Australia had different functional group characteristics than low-S coals, specifically showing increased aliphatic and reduced aromatic functionalities.

With the exception of N content, which is low in the alginite-rich light fractions, there is no regular shift in the proportions of C, O, N, and S in density fractions. The differences in elemental composition among individual macerals result in different elemental ratios. Specifically, the O/C and N/C ratios are highest in corpohuminite, followed by ulminite and alginite, whereas the S/C ratio is highest in alginite, followed by corpohuminite and ulminite.

These elemental data document the large differences between alginite and huminite macerals (corpohuminite and ulminite). Lower O/C and N/C and much higher S/C ratios in alginite may result from differences in original biomass as well as different ability to incorporate sulfur during diagenesis. The alginite S/C ratio of 0.17 to 0.18 (Table 5) significantly exceeds even that of alginite from very high-sulfur Type II-S kerogen. For example, S/C of 0.036 and 0.028 was documented for alginite from the Duwi Formation (Campanian/Maastrichtian, Egypt) and the Monterey Formation (Miocene, California), respectively (Stankiewicz *et al.*, 1996). This very high C/S ratio suggests that, in addition to its original high-sulfur content, the alginite of the coal studied might have experienced the incorporation of significant amounts of sulfur during early diagenesis (Stankiewicz *et al.*, 1997).

CONCLUSIONS

i) For the Oligocene Mequinenza (Spain) lignite studied, the density of liptinite dominated by alginite is below 1.26g/cm^3 (particularly the <1.18g/cm^3), the density of liptinite dominated by a mixture of alginite and other liptinite has a range of 1.26-1.32g/cm^3, the density of the huminite/liptinite mix is 1.32-1.43g/cm^3, and a fraction with more than 93% huminite (textinite/ulminite) has density of 1.43-~1.50g/cm^3. Comparing these density ranges to coals from other locations demonstrates that densities of maceral groups can shift in response to rank, composition of individual macerals within maceral groups and, likely, other local factors.

ii) In-situ elemental analysis of macerals in this coal indicates that alginite has the largest carbon content (75.6% on average) and smallest oxygen content (6.1% on average).

Corpohuminite is characterized by the smallest carbon content (62.3% on average) and the largest oxygen content (21.5% on average). Nitrogen content is similar for corpohuminite and ulminite (~1%), but is significantly lower in alginite (0.2% on average). These are high-organic sulfur coals and sulfur content is high in all the macerals analyzed. Among macerals, sulfur content is greatest in alginite (13.4% on average), followed by corpohuminite (9.8%) and ulminite (7.7%). We suggest that, in addition to the inherent high sulfur content, the alginite of the coal studied experienced the incorporation of additional sulfur during early diagenesis.

iii) Functional group analysis documents expected differences between macerals of huminite and liptinite groups, but also indicates differences between individual macerals within both the huminite and liptinite groups.

TABLE 4 Microprobe elemental analyses (in weight %) of selected macerals in the bulk coal and density fractions. Each value is an average of 5 to 25 analyses and values in brackets are standard deviations

Elements	Macerals		
	Corpohuminite	Ulminite	Alginite
Bulk sample			
C	62.07 (1.41)	67.94 (2.01)	nd
O	21.46 (1.45)	17.90 (1.66)	nd
N	0.85 (0.44)	0.74 (0.45)	nd
Fe	0.04 (0.03)	0.05 (0.05)	nd
Ca	0.84 (0.10)	0.69 (0.04)	nd
Cl	0.11 (0.13)	0.14 (0.02)	nd
S	9.82 (0.28)	7.53 (0.25)	nd
Other	4.81 (0.98)	5.02 (0.19)	nd
Density fraction of 1.00-1.18 g/cm^3			
C	63.33 (2.15)	68.59 (0.10)	72.53 (1.55)
O	20.05 (0.66)	17.56 (0.40)	7.95 (1.56)
N	0.91 (0.46)	0.96 (0.24)	0.22 (0.24)
Fe	0.07 (0.04)	0.04 (0.06)	0.00
Ca	0.44 (0.40)	0.14 (0.03)	0.18 (0.04)
Cl	0.09 (0.01)	0.06 (0.02)	0.06 ((0.04)
S	10.11 (0.11)	9.26 (0.23)	13.18 (0.93)
Other	5.02 (1.41)	3.40 (0.03)	6.38 (0.52)
Density fraction of 1.18-1.22 g/cm^3			
C	62.23 (1.03)	71.23 (1.20)	75.44 (2.12)
O	22.18 (1.10)	15.09 (0.60)	4.64 (3.80)
N	1.15 (0.40)	1.35 (0.15)	0.24 (0.21)
Fe	0.01 (0.01)	0.05 (0.01)	0.00
Ca	0.61 (0.39)	0.26 (0.11)	0.11 (0.11)
Cl	0.10 (0.12)	0.01 (0.01)	0.02 (0.03
S	10.04 (0.45)	7.87 (0.40)	13.78 (0.91)
Other	3.70 (1.20)	4.16 (1.20)	5.78(2.20)
Density fraction of 1.22-1.25 g/cm^3			
C	61.83 (0.51)	74.08 (0.55)	76.21 (0.95)
O	21.91 (0.23)	12.38 (1.04)	5.59 (0.85)
N	1.30 (0.05)	1.26 (0.06)	0.28 (0.36)
Fe	0.05 (0.07)	0.03 (0.04)	0.03 (0.05)
Ca	0.59 (0.11)	0.27 (0.04)	0.15 (0.03)
Cl	0.00	0.04 (0.06)	0.10 (0.07)
S	9.49 (0.05)	7.47 (0.10)	13.13 (0.15)
Other	4.85 (0.45)	4.48 (0.59)	4.54 (0.72)
Density fraction of >1.25 g/cm^3			
C	61.99 (2.02)	68.11 (2.45)	nd
O	21.75 (2.03)	18.82 (2.34)	nd
N	1.54 (0.40)	1.16 (0.36)	nd
Fe	0.00	0.01 (0.01)	nd
Ca	0.45 (0.40)	0.55 (0.06)	nd
Cl	0.15 (0.12)	0.11 (0.14)	nd
S	9.36 (1.66)	6.53 (0.54)	nd
Other	4.75 (1.02)	4.71 (0.79)	nd

These differences are best reflected in aromaticity and hydrocarbon potential, and can be correlated to the reflectance of macerals. Abundance of aliphatic functional groups in vitrinite macerals may relate to the abundance of sulfur in the molecular structure.

ACKNOWLEDGMENTS

We wish to thank Colin Snape, University of Nottingham, for supplying the coal sample. Comments of two reviewers are greatly appreciated.

TABLE 5 | Summary of microprobe analysis in bulk lignite and density fractions (in weight %) and selected elemental ratios

	C	O	N	S	O/C	N/C	S/C
Corpohuminite bulk	62.07	21.46	0.85	9.82	0.346	0.014	0.16
1.0-1.18	63.33	20.05	0.91	10.11	0.317	0.014	0.16
1.18-1.22	62.23	22.18	1.15	10.04	0.356	0.018	0.16
1.22-1.25	61.83	21.91	1.3	9.49	0.354	0.021	0.15
>1.25	61.99	21.75	1.54	9.36	0.351	0.025	0.16
Average	62.29	21.47	1.15	9.764	0.345	0.018	0.16
Ulminite bulk	67.94	17.9	0.74	7.53	0.263	0.011	0.11
1.0-1.18	68.59	17.56	0.96	9.26	0.256	0.014	0.14
1.18-1.22	71.23	15.09	1.35	7.87	0.212	0.019	0.11
1.22-1.25	74.08	12.38	1.26	7.47	0.167	0.017	0.10
>1.25	68.11	18.82	1.16	6.53	0.276	0.017	0.10
Average	69.99	16.35	1.094	7.732	0.235	0.016	0.11
Alginite bulk							
1.0-1.18	75.23	7.97	0.22	13.18	0.106	0.003	0.18
1.18-1.22	75.44	4.64	0.24	13.78	0.062	0.003	0.18
1.22-1.25	76.21	5.59	0.28	13.13	0.073	0.004	0.17
>1.25	na	na	na	na	na	na	na
Average	75.63	6.07	0.25	13.36	0.080	0.003	0.18

REFERENCES

Arenas, C., Luzón, A., Pardo, G., 1999. El Terciaro de Los Monegros: Registro de evolución ambiental en una Cuenca cerrada, In: Melic, A., Blasco-Zumeta, J. (eds.). Manifiesto cientifico por Los Monegros. Boletín de la Sociedad Entomológica Aragonesa (SEA), 24, 51-62.

Bustin, R.M., Mastalerz, M., Wilks, K.R., 1993. Direct determination of carbon, oxygen and nitrogen in coal using the electron microprobe. Fuel, 72, 181-185.

Cabrera, L., Saez, A., 1987. Coal deposition in carbonate-rich shallow lacustrine systems: The Calaf and Mequinenza sequences (Oligocene, eastern Ebro basin, NE Spain. Journal of the Geological Society, 144, 451-461.

Cabrera, L., Cabrera, M., Gorchs, R., De Las Heras, F.X.C., 2002. Lacustrine basin dynamics and organosulphur compound origin in a carbonate-rich lacustrine system (late Oligocene Mequinenza formation, SE Ebro basin, NE Spain). Sedimentary Geology, 148, 289-317.

Chou, C.L., 2012. Sulfur in coals: A review of geochemistry and origins. International Journal of Coal Geology, 100, 1-13.

Drobniak, A., Mastalerz, M., 2006. Chemical evolution of Miocene wood: Example from the Belchatow brown coal deposit, central Poland. International Journal of Coal Geology, 66, 157-178.

Dyrkacz, G.R., Bloomquist, C.A.A., Horwitz, E.P., 1981. Laboratory scale separation of coal macerals. Separation Science and Technology, 16, 1571-1588.

Dyrkacz, G.R., Bloomquist, C.A.A., Solomon, P.R., 1984. Fourier transform infrared study of high-purity maceral types. Fuel, 63, 536-542.

Dyrkacz, G.R., Bloomquist, C.A.A., Ruscic, L., 1991. An investigation of the vitrinite maceral group in microlithotypes using density gradient separation methods. Energy and Fuels, 5, 155-163.

Gurba, L.W., Ward, C.R., 2000. Elemental composition of coal macerals in relation to vitrinite reflectance, Gunnedah Basin, Australia, as determined by electron microprobe analysis. International Journal of Coal Geology, 44, 127-149.

Hower, J.C., Taulbee, D.N., Rimmer, S.M., and Morrell, L.G., 1994. Petrographic and geochemical anatomy of lithotypes from the Blue Gem coal bed, southeastern Kentucky. Energy Fuels, 8, 719-728.

Kister, J., Guiliano, M., Largeau, C., Derenne, S., Casadevall, E., 1990. Characterization of chemical structure, degree of maturation and oil potential of Torbanites (type I kerogens) by quantitative FT-i.r. spectroscopy. Fuel, 69, 1356-1361.

Li, Z., Ward, C.R., Gurba, L.W., 2007. Occurrence of non-mineral inorganic elements in low-rank coal macerals as shown by electron microprobe element mapping techniques. International Journal of Coal Geology, 70, 137-149.

Li, Z., Fredericks, P.M., Ward, C.R., Rintoul, L., 2010. Chemical functionalities of high and low sulfur Australian coals: A case study using micro attenuated total reflectance – Fourier transform infrared (ATR-FTIR) spectrometry. Organic Geochemistry, 41, 554-559.

Lin, R., Ritz, G.P., 1993. Studying individual macerals using i.r. microspectroscopy, and implications on oil versus gas/condensate proneness and "low-rank" generation. Organic Geochemistry, 20, 695-706.

Mastalerz, M., Bustin, R.M., 1993. Variation in maceral chemistry within and between coals of varying rank: an

electronic microprobe and micro-Fourier transform infra-red investigation. Journal of Microscopy, 171, 153-166.

Mastalerz, M., Bustin, R.M., 1996. Application of reflectance micro-Fourier Transform infrared analysis to the study of coal macerals: an example from the Late Jurassic to Early Cretaceous coals of the Mist Mountain Formation, British Columbia, Canada. International Journal of Coal Geology, 32, 55-67.

Mastalerz, M., Gurba, L.W., 2001. Determination of nitrogen in coal macerals using electron microprobe techniques – experimental procedure. International Journal of Coal Geology, 47, 23-30

Mastalerz, M., Schimmelmann, A., Lis, G., Drobniak, A., Stankiewicz, A., 2012. Influence of maceral compositions on geochemical characteristics of immature shale kerogen: Insights from density fraction analysis. International Journal of Coal Geology, 103, 60-69.

Painter, P.C., Starsinic, M., Coleman, M.M., 1985. Determination of functional groups in coal by Fourier transform interferometry. In: Ferraro, J.R., Basile, L.J. (eds.). Fourier Transform Infrared Spectroscopy. New York, Academic Press, 169-240.

Querol, X., Cabrera, L., Pickel, W., López-Soler, A., Hagemann, H. W., Fernández-Turiel, J.L., 1996. Geological controls on the coal quality of the Mequinenza subbituminous coal deposit, northeast Spain. International Journal of Coal Geology, 29, 67-91.

Rimmer, S.M., Rowe, H.D., Taulbee, D.N., Hower, J.C., 2006. Influence of maceral content on $\delta^{13}C$ and $\delta^{15}N$ in a Middle Pennsylvanian coal. Chemical Geology, 225, 77-90.

Robl, T.L., Taulbee, D.N., Barron, L.S., Jones, W.C., 1987. Petrologic chemistry of a Devonian type II kerogen. Energy Fuels, 1, 507-513.

Stankiewicz, B.A., Kruge, M.A., Mastalerz, M., 1996. A study of constituent macerals of Miocene and Eocene coals from Indonesia: implications for the origin of aliphatic-rich vitrinite and resinite. Organic Geochemistry, 24, 531-545.

Stankiewicz, B.A., Mastalerz, M., Kruge, M.A., van Bergen, P.F., Sadowska, A., 1997. A comparative study of modern and fossil cone scales and seeds of conifers: a geochemical approach. New Phytologist, 153, 375-393.

Wagner, M., 1996. Brunatny węgiel bitumiczny ze złóż Turów i Belchatów w swietle badań petrograficzno-chemicznych i sedymentologicznych. PAN Oddzial Krakow Prace Geologiczne, 143, 1-107.

Wang, S.H., Griffiths, P.R., 1985. Resolution enhancement of diffuse reflectance i.r. spectra of coals by Fourier self-deconvolution. 1. C-H stretching and bending modes. Fuel, 64, 229-236.

Ward, C.R., Li, Z., Gurba, L.W., 2005. Variations in coal maceral chemistry with rank advance in the German Creek and Moranbah Coal Measures of the Bowen Basin, Australia, using electron microprobe techniques. International Journal of Coal Geology, 63, 117-129.

White, C.M., Collins, L.W., Veloski, G.A., Irdi, G.A., Rothenberger, K.S., Gray, R.J., LaCount, R.B., Kasrai, M., Bancroft, G.M., Brown, J.R., Huggins, F.E., Shah, N., Huffman, G.P., 1994. A study of Mequinenza lignite. Energy Fuels, 8, 155-171.

Manuscript received December 2012;
revision accepted September 2013;
published Online October 2013.